Analysis of the Turbulent Wake of a Cascade Airfoil

W.A. Gustafson* and D.W. Davis Jr.†
Purdue University, West Lafayette, Ind.
and
F.D. Deffenbaugh‡
Indianapolis Center for Advanced Research, Indianapolis, Ind.

The structure of the wake in an incompressible, turbulent fluid behind an airfoil in a cascade is investigated. Boundary-layer equations containing longitudinal curvature terms are applied to the problem, and the similarity properties of the equations are developed. Local similarity solutions are determined for mean velocity profiles at several wake positions, and these results are compared with experimental data for two incidence angles. Good correlation between theory and experiment is obtained beyond approximately a tenth of a chord downstream of the airfoil at small incidence angles.

I. Introduction

THE structure of a cascade wake has importance in obtaining an understanding of the periodic forces that tend to produce blade vibrations in axial flow compressors. A steady uniform flow entering a stator row is turned by the blades and each blade produces a viscous wake that is usually turbulent and grows in thickness downstream. There are velocity and pressure variations across the wake associated with wake curvature. The rotor blades behind the stator are consequently subjected to a nonsteady, periodic flowfield, which may tend to induce bending and torsional vibration of the blades. These blade vibrations can result in structural failure in certain circumstances.

The analysis presented below considers the development of an incompressible, turbulent, curved wake behind an airfoil, which is part of a cascade. The trailing-edge phenomena as described by Stewartson[1] and Messiter[2] for laminar flow is not considered. The analysis only applies at a downstream location, where mean velocity profiles begin to indicate similarity properties. The existence of similarity has been suggested by the experimental data of Raj and Lakshminarayana.[3] Their data show that the mean velocity profiles indicate weak similarity properties at about a tenth of a chord length downstream from the trailing edge, but the similar nature of the flow increases substantially beyond that point. The correlation of data in Ref. 3 was based on results deduced from similarity considerations applied to the turbulent boundary-layer equation neglecting curvature terms. In addition, one other term in the equation was neglected, which permitted the following results to be obtained. It was shown that $U_e(x) \sim x^{-m}$, $U_c(x)/U_e(x) \sim x^{-(1-m)/2}$, and $b(x) \sim x^{(m+1)/2}$ where U_e is the wake edge velocity, x is the distance downstream from the airfoil trailing edge, U_c is the wake centerline velocity, m is a parameter that depends on various geometric factors, and b is the wake width. The fact that the edge velocity and centerline velocity vary as a power law in downstream distance suggests that a wake analysis might be carried out by means of a similar solution. Also an examination of the experimental mean velocity profiles in Ref. 3 shows an asymmetry in structure, thereby indicating that curvature may be a significant factor and should be included in the analysis.

Received Jan. 22, 1976; revision received Dec. 27, 1976.
Index category: Jets, Wakes, and Viscid-Inviscid Flow Interactions.

*Professor, School of Aeronautics and Astronautics. Member AIAA.
†Graduate Research Assistant, School of Aeronautics and Astronautics.
‡Presently at Systems Group of TRW Inc., Redondo Beach, Calif. Member AIAA.

II. Similarity Analysis of the Boundary-Layer Equations

It is assumed that the incompressible, turbulent, curved wake behind an airfoil in a cascade can be described by means of the appropriate boundary-layer approximation of the Navier-Stokes equations. An orthogonal curvilinear coordinate system is used in which the x direction corresponds to the wake "centerline," and the y direction is everywhere normal to it. The wake "centerline" is more clearly defined as the locus of the minimum points of the mean velocity profiles in the wake. Transformation of the Navier-Stokes equations in Cartesian coordinates to this curvilinear coordinate system is given by Goldstein.[4] The subsequent order of magnitude analysis that retains first-order longitudinal curvature effects is given by Schultz-Grunow and Breuer[5] for laminar flow. An equivalent procedure can also be done for turbulent flow as indicated by Spence,[6] and the results for the continuity and momentum equations ignoring viscous stresses are

$$\frac{\partial u}{\partial x} + \frac{\partial}{\partial y}[(1+ky)v] = 0 \tag{1}$$

$$\frac{1}{1+ky}u\frac{\partial u}{\partial x} + v\frac{\partial u}{\partial y} + \frac{kuv}{1+ky} + \frac{1}{\rho(1+ky)}\frac{\partial p}{\partial x} = \epsilon\frac{\partial^2 u}{\partial y^2} + \frac{2k\epsilon}{1+ky}\frac{\partial u}{\partial y} \tag{2}$$

$$\frac{1}{\rho}\frac{\partial p}{\partial y} = \frac{ku^2}{1+ky} \tag{3}$$

where $p(x,y)$ is the pressure, u and v are the mean trubulent velocity components, $k(x)$ is the curvature, and the Reynolds stress has been replaced by an eddy viscosity law, i.e., $-\overline{u'v'} \equiv \epsilon\partial u/\partial y$, where $\epsilon(x)$ is the eddy viscosity that we will assume in general is a function of x. Note that these "higher order" boundary-layer momentum equations have both an x and a y component, the second one stating that a pressure gradient exists across the boundary layer due to the curvature of the flow. These equations can be solved for $u(x,y)$, $v(x,y)$, and $p(x,y)$ assuming that $k(x)$ and $\epsilon(x)$ are specified, and that appropriate boundary conditions are given. The wake "centerline" is that line along which the velocity at any position x has its minimum value. Thus $k(x)$ describes the curvature of this line ($y=0$) along which we apply boundary conditions such that $\partial u/\partial y = 0$ and $v = 0$. The outer edge of the wake should merge into an inviscid flow determined from the cascade geometry. This solution is not available for the cascade used in the experiments of Ref. 3, so we will use a boundary condition obtained by requiring that the outer flow

be irrotational. The form of this boundary condition is discussed at a later point in the presentation.

The next step in the analysis is to eliminate $p(x,y)$ from Eqs. (2) and (3) by cross differentiation, and then replace u and v in terms of the stream function $\psi(x,y)$, which can be introduced to satisfy the continuity equation as follows.

$$u=\frac{\partial\psi}{\partial y} \qquad v=-\frac{1}{1+ky}\frac{\partial\psi}{\partial x} \tag{4}$$

Carrying out these manipulations produces the stream-function equation

$$\psi_y\psi_{xyy}-\psi_x\psi_{yyy}-\frac{k}{1+ky}\psi_x\psi_{yy}+\frac{k}{1+ky}\psi_y\psi_{xy}+\frac{k_x}{(1+ky)^2}\psi_y^2$$
$$+\frac{k^2}{(1+ky)^2}\psi_x\psi_y=\epsilon(1+ky)\psi_{yyyy}+3k\epsilon\psi_{yyy} \tag{5}$$

where subscripts x and y denote partial differentiation.

We are now ready to investigate the possibility of similar solutions to the turbulent, incompressible wake with curvature. This is carried out in a way similar to that done by Massey and Clayton[7] for laminar flows with curvature. We define the following dimensionless forms for the variables

$$\eta=\frac{Y\sqrt{Re}}{Lg(x)} \qquad \psi=\frac{Lg(x)}{\sqrt{Re}}[U_0(x)f(\eta)+U_e(x)\eta]$$
$$k(x)=\frac{\sqrt{Re}\,\Omega}{Lg(x)} \qquad \epsilon(x)=\epsilon_0(x/L)^s$$
$$Re=\frac{U_{el}L}{\epsilon_0} \qquad U_0(x)=U_e(x)-U_c(x) \tag{6}$$

where L is a characteristic length (airfoil chord), ϵ_0 is a constant, Ω is a dimensionless curvature parameter, U_{el} is the wake edge velocity at the airfoil trailing edge, $U_e(x)$ is the wake edge velocity, $U_c(x)$ is the minimum velocity in the wake at $y=0$, η is the new independent variable, and $f(\eta)$ is the dependent variable. This definition of ψ gives the velocity u as

$$u=\frac{\partial\psi}{\partial y}=U_0f'+U_e \tag{7}$$

and substitution for U_0 gives

$$(u-U_e)/(U_e-U_c)=f' \tag{8}$$

The transformation relations (6) are substituted into Eq. (5) and after some algebraic manipulation we obtain

$$(1+\Omega\eta)^3f''''+3\Omega(1+\Omega\eta)^2f'''+k_1[(1+\Omega\eta)^2ff'''$$
$$+\Omega(1+\Omega\eta)ff''-\Omega^2ff']+k_2[(1+\Omega\eta)^2\eta f'''$$
$$+\Omega(1+\Omega\eta)\eta f'']$$
$$-k_3[(1+\Omega\eta)^2f'f''+\Omega(1+\Omega\eta)f'^2]$$
$$-k_4\eta\Omega^2f'-k_5(1+\Omega\eta)^2f''-k_6\Omega^2f$$
$$-k_7\Omega(1+\Omega\eta)f'-k_8[\Omega(1+\Omega\eta)+\Omega^2\eta]$$
$$+k_9\Omega f'+k_{10}\Omega=0 \tag{9}$$

where coefficients k_1 to k_{10} are all functions of x, and therefore each must be a constant in order to obtain a similarity solution. The form of these coefficients is given below.

$$k_1=\frac{L}{U_{el}}=\frac{g}{(x/L)^s}(U_0g)'$$
$$k_2=\frac{L}{U_{el}}\frac{g}{(x/L)^s}(U_eg)'$$
$$k_3=\frac{L}{U_{el}}\frac{g^3}{(x/L)^s}\left(\frac{U_0}{g}\right)'$$
$$k_4=\frac{L}{U_{el}}\frac{g^3}{(x/L)^s}\left(\frac{U_e}{g}\right)'$$
$$k_5=\frac{L}{U_{el}}\frac{g^3}{(x/L)^s}\frac{U_e}{U_0}\left(\frac{U_0}{g}\right)'$$
$$k_6=\frac{L}{U_{el}}\frac{g}{(x/L)^s}\frac{U_e}{U_0}(U_0g)'$$
$$k_7=\frac{L}{U_{el}}\frac{g^2}{(x/L)^s}\left(\frac{(U_0U_e)'}{U_0}\right)$$
$$k_8=\frac{L}{U_{el}}\frac{g^2}{(x/L)^s}\frac{U_eU_e'}{U_0}$$
$$k_9=\frac{L}{U_{el}}\frac{2g}{(x/L)^s}U_eg'$$
$$k_{10}=\frac{L}{U_{el}}\frac{g}{(x/L)^s}\frac{U_e^2g'}{U_0} \tag{10}$$

Comparing k_1 and k_2 it can be seen that U_0 and U_e must be of the same functional form. Since $U_0=U_e-U_c$, it is clear that U_c must also be of the same form, namely a power function of x with the same exponent. However, this does not conform to the physical situation of the wake behind an airfoil in a cascade. As Ref. 3 indicates, the edge velocity $U_e\sim x^{-m}$, i.e., it is retarded, whereas the "centerline" velocity must increase at a different rate corresponding to a different exponent. Hence, a similarity solution is not possible for this wake problem unless some assumptions based on experimental data can be made. In Ref. 3, it was assumed and then verified from the data (see Fig. 4, Ref. 3) that the product U_0g is a constant in the wake. Adoption of this result gives $k_1=k_6=0$, $k_5=-k_9=k_4-k_2$, $k_7=k_4$, $k_8=(k_4^2-k_2^2)/2k_3$, $k_{10}=-(k_2-k_4)^2/2k_3$, where

$$k_0=U_0g \tag{11}$$
$$k_2=\frac{L}{U_{el}}\frac{g}{(x/L)^s}(U_eg)'\equiv\alpha \tag{12}$$
$$k_3=\frac{L}{U_{el}}\frac{g^3}{(x/L)^s}\left(\frac{U_0}{g}\right)' \tag{13}$$
$$k_4=\frac{L}{U_{el}}\frac{g^3}{(x/L)^s}\left(\frac{U_e}{g}\right)'\equiv\gamma \tag{14}$$

The coefficients have now been reduced to a set of four primary coefficients k_0, k_2, k_3, k_4, plus five others expressed in terms of k_2, k_3, and k_4. The coefficients k_0, k_2, k_3, and k_4 can be shown to be exactly the same as those discussed in Ref. 3, accounting for differences in notation and taking $s=0$ which means that $\epsilon=$ constant. In Ref. 3 the coefficient k_3 was neglected by assuming that it appeared in a term in the differential equation which was negligible. If one compares k_3

and k_4, it is evident that these two coefficients require that U_0 and U_e be proportional, which again makes it impossible to obtain a similarity solution that would be consistent in structure with the wake problem that we are trying to solve. Hence, two approaches to the problem are now possible. We can neglect k_3, which also requires that we neglect k_8 and k_{10}, and then it is possible to obtain a global similarity solution. Alternatively, we could proceed by means of a local similarity solution. This involves choosing several downstream locations in the wake and evaluating the coefficients at those values of x, then solving the differential equations at each of these locations. The wake structure can then be patched together from these solutions. We follow the later procedure retaining k_3, k_8, and k_{10}, and proceeding with the solution of Eqs. (12) and (14), in a manner similar to that given in Ref. 7 for the laminar case, obtaining

$$g=\left[\frac{(3\alpha-\gamma)}{2(s+1)}\left(\frac{x}{L}\right)^{s+1}\frac{U_{et}}{U_e}\right]^{1/2} \tag{15}$$

and

$$\frac{U_e}{U_{et}}=C_2{}^{2/(3\alpha-\gamma)}\left[\frac{(3\alpha-\gamma)}{2(s+1)}\left(\frac{x}{L}\right)^{s+1}\right]^{(\alpha+\gamma)/(3\alpha-\gamma)} \tag{16}$$

At this point we can set $\alpha=1$ without loss of generality since, in Eq. (12), α can be absorbed into a redefined $g(x)$. The case $\alpha=0$ is a special case and will not be considered here. With $\alpha=1$ we have

$$U_e/U_{et}=C_2{}^{2/(3-\gamma)}\left[\frac{(3-\gamma)}{2(s+1)}\right]^{(1+\gamma)/(3-\gamma)}\times\left(\frac{x}{L}\right)^{(s+1)(1+\gamma)/(3-\gamma)} \tag{17}$$

$$g=\left[\frac{(3-\gamma)}{2(s+1)}\right]^{(1-\gamma)/(3-\gamma)}C_2{}^{-1/(3-\gamma)}\times\left(\frac{x}{L}\right)^{(s+1)(1-\gamma)/(3-\gamma)} \tag{18}$$

Experimentally we know that U_e and U_0 must vary as a different power function of x; hence, dividing Eq. (11) by Eq. (17) and using Eq. (18) gives

$$\frac{U_0}{U_e}=\frac{k_0}{U_{et}}C_2{}^{-1/(3-\gamma)}\left[\frac{3-\gamma}{2(s+1)}\right]^{-2/(3-\gamma)}\left(\frac{x}{L}\right)^{-2(s+1)/(3-\gamma)} \tag{19}$$

The remaining transformations become

$$\eta=\frac{y}{L}\sqrt{Re}\,C_2{}^{1/(3-\gamma)}\left[\frac{3-\gamma}{2(s+1)}\right]^{-(1-\gamma)/(3-\gamma)}\times\left(\frac{x}{L}\right)^{-(s+1)(1-\gamma)/(3-\gamma)} \tag{20}$$

$$k=\Omega\left[\frac{2(s+1)}{3-\gamma}\,\frac{1}{(x/L)^s}\,\frac{U_e}{mx}\right]^{1/2} \tag{21}$$

Based on the foregoing analyses, the boundary-value problem for local similarity now becomes

$$(1+\Omega\eta)^3f''''+(1+\Omega\eta)^2[3\Omega f'''+\eta f'''+f'']+\Omega(1+\Omega\eta)\eta f''+\Omega f'-\gamma[(1+\Omega\eta)^2f''+2\Omega^2\eta f'+2\Omega f']=k_3[(1+\Omega\eta)^2f'f''+\Omega(1+\Omega\eta)f'^2]-[\Omega(1-\gamma)/k_3][\gamma+(1-\gamma)\Omega\eta]$$

$$f(0)=f''(0)=0 \qquad f'(0)=-1$$

$$f'(\pm\infty)=-\Omega\eta/(1+\Omega\eta) \tag{22}$$

Note that k_3 must be evaluated at each downstream location x, and Eq. (22) must be solved at each station.

The boundary condition on $f'(\eta)$ as η becomes large comes from assuming that the wake merges with an outer irrotational flow. In the coordinate system being used here the vorticity is

$$\zeta=\frac{1}{1+ky}\frac{\partial v}{\partial x}-\frac{\partial}{\partial y}[(1+ky)u] \tag{23}$$

At high Reynolds numbers, the wake is thin and we can neglect $\partial v/\partial x$ compared to the other terms. In defining the similarity variables, it should be noted that the wake velocity profile as given by $f'(\eta)$ only accounts for the change in velocity from the "centerline" value U_c to the outer edge velocity U_e. It was necessary to define the transformation this way because $U_e(x)$ and $U_c(x)$ are different functions, so in effect we subtracted the "centerline" velocity from the total wake velocity so that $f'(\eta)$ will not involve x at the boundaries. Therefore, in Eq. (23), we neglect the first term, set $\zeta=0$, and also substract U_c from u to give

$$\frac{\partial}{\partial y}[(1+ky)(u-U_c)]=0 \tag{24}$$

Integrating we obtain $u-U_c=G(x)/(1+ky)$ where $G(x)$ is a function of integration which can now be chosen to give a proper form to the boundary condition in similarity variables. From Eq. (7) we can sutstitute for u, and choosing $G(x)=U_0(x)$ we get for large η

$$f'=1/(1+\Omega\eta)-1=-\Omega\eta/(1+\Omega\eta) \tag{25}$$

This type of boundary condition has been used in several boundary-layer analyses[5,7,8] in which longitudinal curvature is considered and reflects the fact that the outer flow has a velocity variation at a given point x because of its curvature.

Since we later make some comparison of results of local similarity and global similarity, it is necessary to indicate the difference in these methods in terms of the equations. For global similarity, we neglect the terms in Eq. (9) that contain k_3, k_8, and k_{10}, and thus the remaining coefficients are $k_1=k_6=0$, $k_2=\alpha=1$, $k_7=k_4=\gamma$, $k_5=\gamma-1$, and $k_9=1-\gamma$. The resulting differential equation is

$$(1+\Omega\eta)^3f''''+(1+\Omega\eta)^2[3\Omega f'''+\eta f'''+f'']+\Omega(1+\Omega\eta)\eta f''+\Omega f'-\gamma[(1+\Omega\eta)^2f''+2\Omega(1+\Omega\eta)f']=0 \tag{26}$$

with the same boundary conditions previously given. Here it is noted that γ is a constant for a given flow condition, and hence the solution to this equation applies at any wake location.

III. Eddy Viscosity and Parameter Determination

The classical expression for eddy viscosity as applied to problems in free turbulence is

$$\epsilon=\epsilon_0 b(x)[u_{\max}(x)-U_{\min}(x)]=\epsilon_0 b(x)U_0(x) \tag{27}$$

where ϵ_0 is a constant, $b(x)$ is a measure of the wake width, and in this case the velocity difference is just $U_0(x)$.

Our primary interest with this analysis is in comparing it with the experimental data of Ref. 3 where it is shown that

$$b(x)\sim(x/L)^p \tag{28}$$

where $p=0.58$ for all three incidence angles considered, namely $i=0$, 2, and -6 deg. In our similarity analysis, we represented $\epsilon(x)$ as shown in Eq. (6), which must be consistent with Eq. (28). Hence, using Eqs. (6), (11), and (27) we have

$$\epsilon=\epsilon_0(x/L)^s=\epsilon_0 b(x)U_0(x)\sim(x/L)^p \cdot(x/L)^{-(s+1)(1-\gamma)/(3-\gamma)} \tag{29}$$

It is clear that p must be represented in terms of s and γ as follows

$$p=s+(s+1)(1-\gamma)/(3-\gamma) \tag{30}$$

and s and γ must have values such that $p=0.58$. Another condition is clearly required in order to determine s and γ uniquely.

In Ref. 3, the wake edge velocity is correlated in the form $U_e(x)\sim x^{-m}$ where m has a specified value for each of the three incidence angles investigated. The form of U_e is given by Eq. (17); thus we have

$$(s+1)(1+\gamma)/(3-\gamma)=-m \tag{31}$$

The evaluation of s and γ can now be determined uniquely using Eqs. (30) and (31) since a given set of experimental data specify the value of m and p. Solving these two equations gives

$$s=(2p-1-m)/3 \qquad \gamma=(4m+p+1)/(2m-p-1) \tag{32}$$

The integration of Eq. (22) can now be accomplished upon input of the wake curvature parameter Ω and k_3. Substitution of Eqs. (11) and (18) into Eq. (13) permits k_3 to be written as

$$k_3=\frac{-2k_0}{U_{et}}\left[(3-\gamma)/2(s+1)\right]^{(1-\gamma)/(3-\gamma)} \times C_2^{-1/(3-\gamma)}\frac{(s+1)(1-\gamma)}{(3-\gamma)}(x/L)^{-2(s+1)/(3-\gamma)} \tag{33}$$

where the constants k_0/U_{et} and C_2 are obtained from Eqs. (17) and (19) by matching U_e/U_{et} and $U_0/U_e=1-U_c/U_e$ with the corresponding experimental data of Ref. 3, which is also shown in Figs. 1 and 2. In Ref. 3 the data for U_e/U_{et} and U_0/U_e as a function of downstream distance x was put on a log-log plot and a straight line correlation was used. Thus one could write that $U_e/U_{et}=Ax^B$ and a similar expression for U_0/U_e. We have made a slight revision in this correlation as shown in Figs. 1 and 2, where the experimental points and correlation of Ref. 3 are shown along with a new least-squares fit of the data with a function of the form Ax^B. The coefficient A and exponent b are slightly different than those given in Ref. 3 and we believe that the new correlation is more accurate. It should be noted that the correlation for $i=-6$ deg is slightly poorer than at the other incidence angles $i=0$ deg and $i=2$ deg, hence, we should expect that the final results for velocity profiles would be poorest for this case.

A summary of the parameter values needed to solve Eq. (22) as obtained by correlation with experimental data is given in Table 1. Although we have kept p a constant as suggested in Ref. (3), there is no restriction in the theory that requires this.

Table 1 Parameter values

i, deg	m	p	γ	s	C_2	k_0/U_{et}
2	0.0198	0.58	−1.077	0.0467	0.864	0.156
0	0.0473	0.58	−1.191	0.0376	0.727	0.166
−6	0.1157	0.58	−1.515	0.0148	0.396	0.209

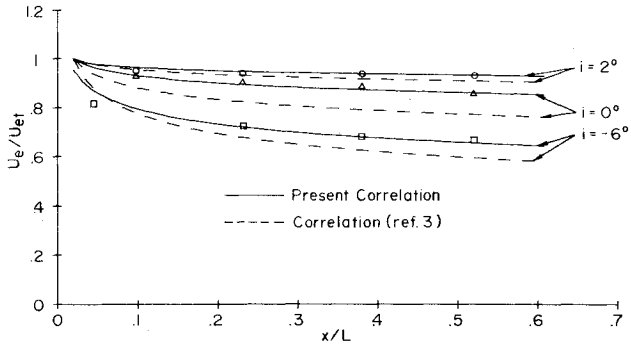

Fig. 1 Variation of wake edge velocity with downsteam distance. Experimental data points from Ref. 3.

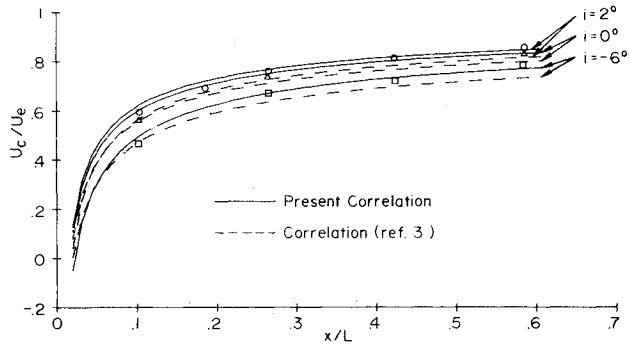

Fig. 2 Variation of wake centerline velocity with downstream distance. Experimental data points from Ref. 3.

The wake curvature as represented by the shape of the x axis can be determined from the curvature expression in Eq. (6) as follows.

$$k=\frac{\sqrt{R_e}}{L}\frac{\Omega}{g(x)}\equiv-\frac{d\phi}{dx} \tag{34}$$

where ϕ is the angle between a tangent to the x axis and the direction of the cascade axis. Substituting Eq. (18) into Eq. (34) and integrating with respect to x yields

$$\phi=\phi_1-R_e^{1/2}\Omega C_2^{1/(3-\gamma)}\frac{(3-\gamma)}{[2-s(1-\gamma)]} \times\left[\frac{3-\gamma}{2(s+1)}\right]^{(\gamma-1)/(3-\gamma)}\left(\frac{x}{L}\right)^{\{2-s(1-\gamma)\}/(3-\gamma)} \tag{35}$$

where ϕ_1 is the value of ϕ at $x=0$, i.e., ϕ_1 defines the direction of the flow leaving the trailing edge of the airfoil relative to the cascade axis. To calculate the shape of the x axis, it is convenient to determine (X, Y) coordinates where X is in the direction of the cascade axis, and Y is perpendicular to the cascade axis and directed along a line through the trailing edge of each airfoil. Thus $X=\int\cos\phi dx$ and $Y=\int\sin\phi dx$, with the integration starting from the airfoil trailing edge. These integrations must be done numerically.

IV. Numerical Integration

The "triple point" boundary value problem (22) is solved using a "shooting" method. The solution must satisfy boundary conditions at the edge of the wake as well as three boundary conditions along the centerline. However, since the governing differential equation (22) is of fourth order, four boundary conditions are all that is required to completely determine the solution. It is convenient to start the numerical

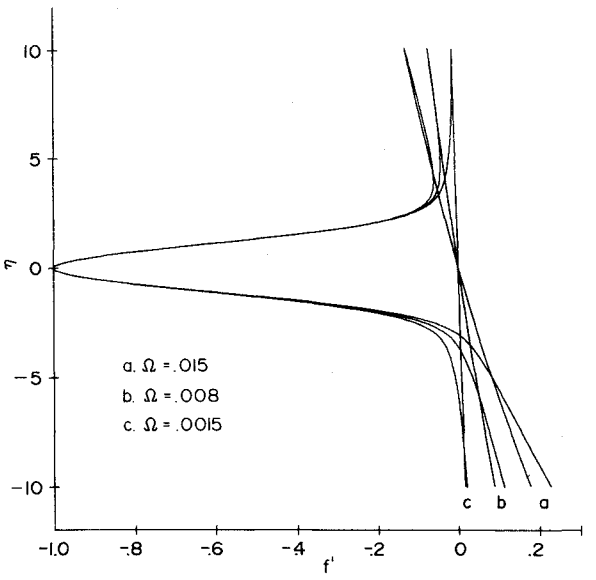

Fig. 3 Local similarity solution, $i = 0$ deg, $x/L = 0.08$, $R_e = 900$.

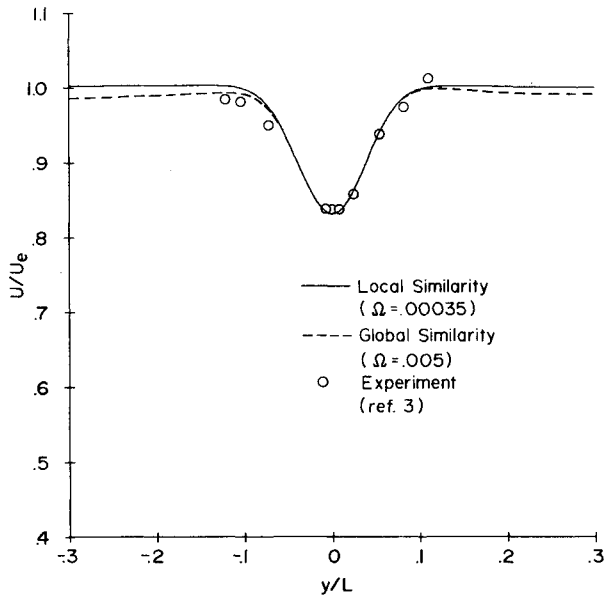

Fig 4 Mean velocity profile, $i = 0$ deg, $x/L = 0.56$, $R_e = 900$.

integration of the differential equation at $\eta = 0$ where the greatest number of boundary conditions are specified. The fourth boundary condition is arbitrarily chosen to be the one at $\eta = +\infty$. Once the boundary-value problem has been solved for positive η, then the solution for negative values of η is determined and easily obtained.

The boundary-value problem is transformed into an initial value problem by guessing the initial value of $f'''(0)$. The numerical integration is then started at $\eta = 0$ with the given values of $f(0) = 0$, $f'(0) = -1$, $f''(0) = 0$, and the assumed value of $f'''(0)$. A value of Ω is selected and k_3 is determined for the chosen downstream location x/L. The integration is carried out to some value of η where it is assumed that the outer boundary conditions are satisfied. This value of η is denoted as η_s. For the present problem $\eta_s = 7.0$. At the outer limit the computed value of $f'(\eta_s)$ is compared with the required boundary condition.

The computed value of $f''(\eta_s)$ is also compared with the required value of $f''(\eta_s)$ which is obtained by differentiating the second boundary condition of Eq. (22). Based on the resulting errors at the outer limit, a new value of $f'''(0)$ is chosen and the integration is repeated. When the conditions of $f'(\eta_s)$ and $f''(\eta_s)$ are satisfied to within some specified error the integration procedure stops. This procedure is based on a method developed by Nachtsheim and Swigert.[9] The integration is then carried out to $\eta = -\eta_s$, using the current value of $f'''(0)$ to complete the wake solution. If the initial choice of Ω was not proper, then the solution for negative η will not merge with the proper value for the outer irrotational flow boundary condition. It is then necessary to start over with a new value of Ω and repeat the process until a value of Ω is found such that f' approaches the outer solution for both positive and negative η. This procedure determines the appropriate value of the curvature parameter for the local similarity solution at each downstream station selected. Figure 3 shows a typical result of this process for several values of Ω. Note that for positive η the solution is forced to merge with the outer flow for all Ω, but only for $\Omega = 0.0015$ does the solution for the indicated parameter values satisfy the boundary condition for large negative η. The procedure for determining the wake structure by means of local similarity is to select several downstream locations and solve the differential equation at each location finding the value of Ω so that the solution merges with the outer flow on both sides of the wake. A global similarity solution is found in a different way because there can be only one value of Ω for the entire wake, and hence, one similarity solution applies at all wake locations. The result of this is that one must select an Ω so that the velocity deficit region of the solution has the proper width to correlate the experimental data, but then one finds that the boundary condition for negative η is not satisfied in all cases. It was pointed out in Sec. II that this problem does not have a global similarity solution unless one neglects, without justification, some terms in the equation. The consequences of doing that are now apparent. However, it is shown in the following section that velocity profiles in physical space can be made to correlate the data in the velocity deficit region to a reasonable degree in some cases even with global similarity.

Since the experimental data of Ref. 3 is presented in the form of velocity profiles u/U_e as a function of y/L, it is then necessary to take the results of the similarity solution $f'(\eta)$ and convert it into the physical space variables. This can be done by referring to Eq. (7) and dividing it by U_e. Hence, for a selected downstream location x/L and for a given η the numerical solution gives $f'(\eta)$, and U_0/U_e is obtained from Eq. (19). For the same η, Eq. (20) provides y/L, and hence, it

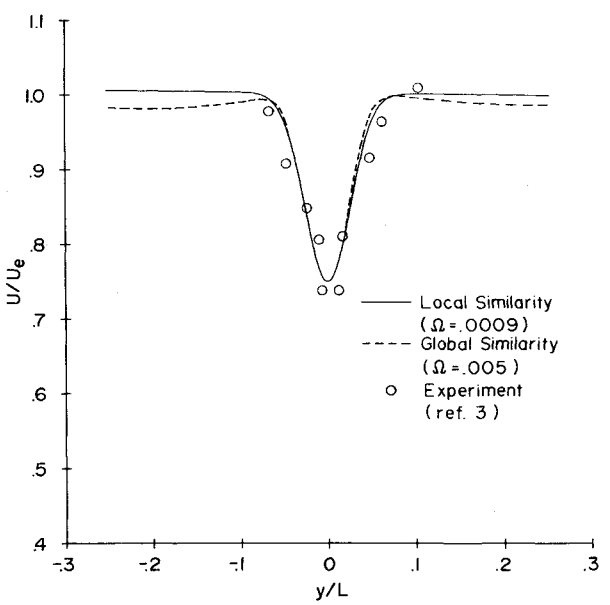

Fig. 5 Mean velocity profile, $i = 0$ deg, $x/L = 0.24$, $R_e = 900$.

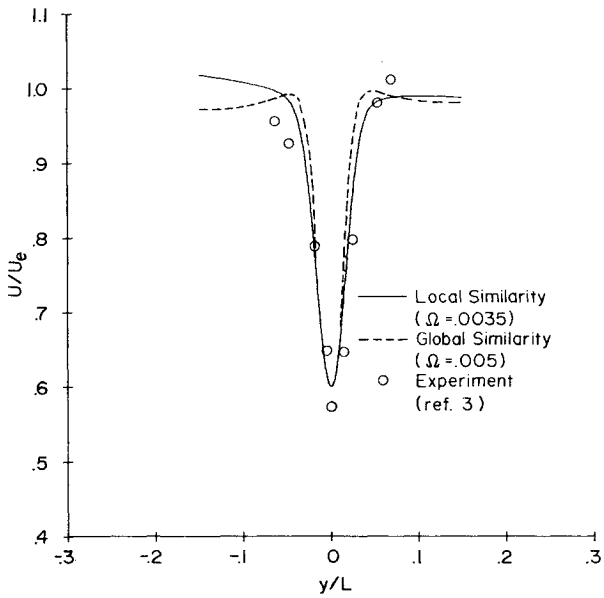

Fig. 6 Mean velocity profile, $i=0$ deg, $x/L=0.08$, $R_e=900$.

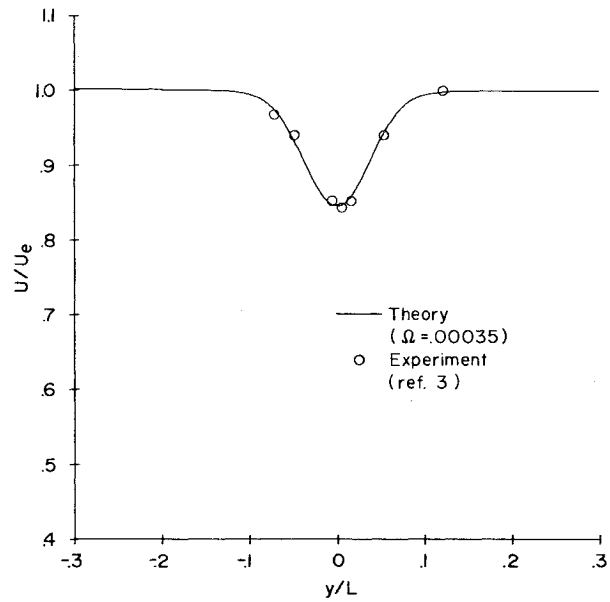

Fig. 7 Mean velocity profile, $i=2$ deg, $x/L=0.56$, $R_e=900$.

is possible to plot u/U_e versus y/L. Note that the turbulent Reynolds number $R_e \equiv U_{el}L/\epsilon_0$ appears in the expression for y/L, and ϵ_0 is the unknown constant in the eddy viscosity relation. Thus, one must arbitrarily select a value for R_2 (or ϵ_0) which gives agreement between theory and experiment, which is a requirement of all turbulence theories.

V. Comparson of Theory and Experiment

Reference 3 gives experimental data for a cascade of fixed geometry and entering velocity, and for three values of incidence angle, $i=2$, 0, and -6 deg. For the incidence angle $i=0$ deg velocity-profile data are provided at three wake locations: $x/L=0.8$, $x/L=0.24$, and $x/L=0.56$ excluding $x/L=0$ which is too near the trailing edge for similarity to apply. These locations are based on a coordinate system whose origin is located at 2% of the airfoil chord downstream of the trailing edge. Figure 4 shows the velocity profiles for both a global and a local similarity solution at $x/L=0.56$. Figures 5 and 6 shown the same results at upstream positions nearer the airfoil trailing edge. The curvature parameter has

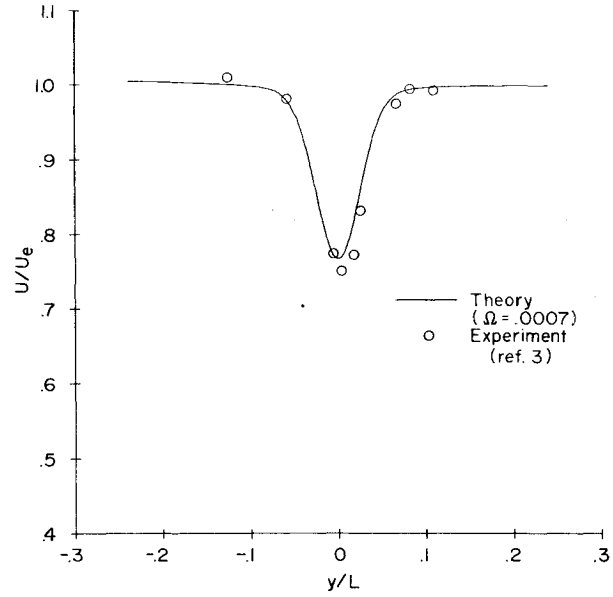

Fig. 8 Mean velocity profile, $i=2$ deg, $x/L=0.24$, $R_e=900$.

been selected for both solutions so that there is agreement in the region of large velocity deficit; however, the global solution does not merge with the boundary condition for large negative η, whereas the local similarity solution agrees well. The numerical results (f' vs η) which were required for these figures is not included in graphical form. Figures 5 and 6 show that the global solution velocity profiles deviate increasingly from the local solution in the velocity deficit region as the trailing edge is approached. In most cases, experimental data are not available at sufficiently large y/L to check agreement between theory and experiment with the outer flow. It is clear that similarity solutions tend to become poorer near the trailiing edge of the airfoil, but the local similarity solution in general gives a better representation of mean velocity profiles than does global similarity. The results of Fig. 6 are reasonably good considering that this location is just 10% of the chord behind the trailing edge. It should be observed that Ω has its largest value near the airfoil trailing edge and decreases downstream. Thus the wake is curved most just behind the airfoil, but tends to straighten downstream. Global similarity requires a constant curvature parameter that is not realistic.

The velocity profiles for the incidence angle $i=2$ deg are shown in Figs 7-9, and again the corresponding similarity solutions (f' vs η) have not been plotted nor are global similarity results shown. In general, the comparison of theory and experiment for both $i=0$ deg and $i=2$ deg is quite good. This is due to the fact that for these angles both the wake edge velocity and "centerline" velocity follow a power law variation from $x/L=0.1$ downstream very closely as was indicated in Figs. 1 and 2. Also at these angles the blades are not highly loaded and the boundary layers on the blades are quite likely not separated.

Reference 3 includes experimental data for $i=-6$ deg, but in the interests of brevity we have not included any comparison of theory and experiment for this case. In general, the results are poorer for this case than for the two previous cases, although at $x/L=0.56$ agreement is still fairly good. One possible reason for this can be seen in Fig. 1 in that a power law does not correlate the experimental data as well for $i=-6$ deg as for the other two cases, particularly near the trailing edge. Another possibility is that the outer boundary conditions that we have imposed are simply based on an assumed outer irrotational flow, rather then being determined for the particular cascade in question.

Another area in which correlation of theory and experiment is possible has to do with wake curvature. No experimental

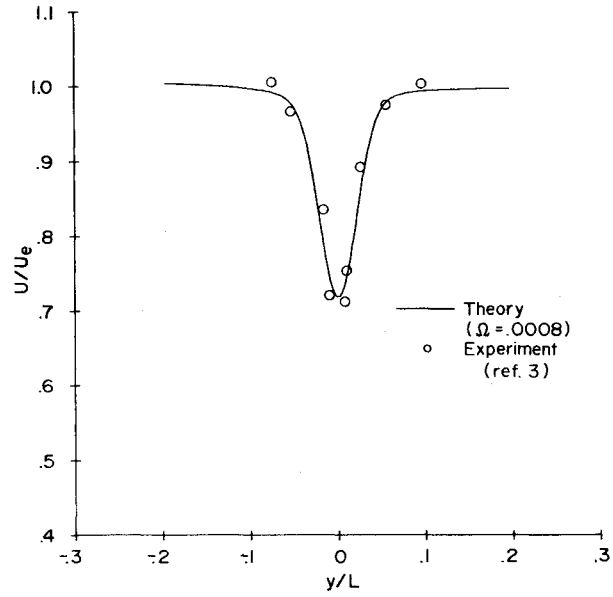

Fig. 9 Mean velocity profile, $i=2$ deg, $x/L=0.16$, $R_e=900$.

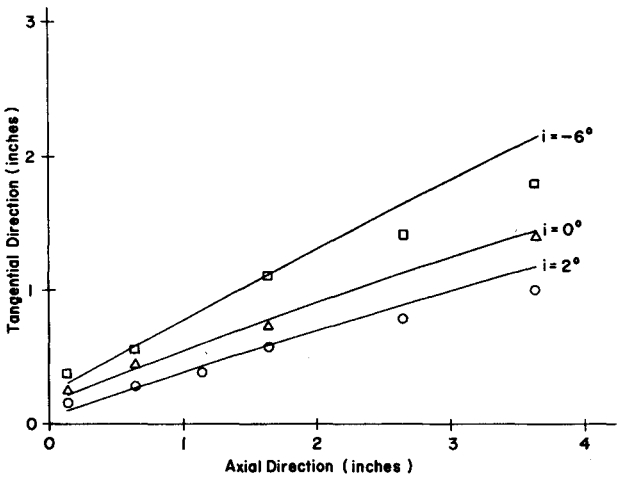

Fig. 10 Locus of minimum velocity points in the wake.

evidence of this aspect of cascade wakes is given in Ref. 3, but Ref. 10 provides the original velocity profiles as measured in physical space. The displacement of the minimum velocity point of each profile relative to the cascade axis is given, so that a line through these points represents wake turning. This line is equivalent to the x axis of the theory, and, hence, a comparison is possible. A numerical integration of $\sin\phi$ and $\cos\phi$ in several parts is required to find X and Y because Ω changes in the downstream direction. Figure 10 shows a comparison of theory and experiment for all three incidence angles. It is evident that wake curvature is not very large and the curvature parameter Ω diminishes in the downstream direction. The lack of agreement is probably due to the difficulty in establishing the initial value of the slope of the wake ϕ_1.

VI. Conclusions

It has been established that a local similarity solution provides good agreement with the available experimental data on mean velocity profiles for a cascade wake in an incompressible, turbulent fluid accounting for curvature effects. The agreement between theory and experiment improves in the downstream direction behind the airfoil, but agreement is reasonably good even at a point which is only 10% of the chord behind the airfoil when the incidence angles are small. In addition, the wake curvature results from theory and experiment correlate well for those cases where velocity profiles correlate. It is also of interest to note that the similarity solution requires a power law variation of the eddy viscosity downstream of the trailing edge, and the exponent has a different value for each incidence angle. This is not an unusual result for similarity solutions of problems in free turbulence. For example, the two-dimensional turbulent jet and the turbulent mixing of two parallel streams of different mean velocities, both have an eddy viscosity that varies in the streamwise direction, and results in good correlation between theory and experiment.

Acknowledgment

This research was supported by the U.S. Air Force Office of Scientific Research under Contract F 44620-74-C-0065, and by the Indianapolis Center for Advanced Research. The authors wish to acknowledge a number of helpful discussions with Dr. G.D. Huffman.

References

[1]Stewartson, K., "On the Flow Near the Trailing Edge of a Flat Plate," *Proceedings of the Royal Society, Series A*, Vol. 306, Sept. 1968, pp. 275-290.

[2]Messiter, A.F., "Boundary Layer Flow Near the Trailing Edge of a Flat Plate," *SIAM Journal of Applied Mathematics*, Vol. 18, Jan. 1970, pp. 241-257.

[3]Raj, R., and Lakshminarayana, B., "Characteristics of the Wake Behind a Cascade of Airfoils," *Journal of Fluid Mechanics*, Vol. 61, Dec. 1973, pp. 707-730.

[4]Goldstein, S., *Modern Developments in Fluid Dynamics*, Vol. 1, Oxford University Press, London, 1938, pp. 119.

[5]Schultz-Grunow, F. and Breuer, W., "Laminar Boundary Layers on Cambered Walls," *Basic Developments in Fluid Dynamics*, Vol. I, M. Holt, ed., Academic Press, New York, 1965.

[6]Spence, D.A., "Wake Curvature and the Kutta Condition," *Journal of Fluid Mechanics*, Vol. 44, Dec. 1970, pp. 625-636.

[7]Massey, B.S. and Clayton, B.R., "Laminar Boundary Layers and Their Separation from Curved Surfaces," *Transactions of the ASME, Journal of Basic Engineering*, Vol. 87, June 1965, pp. 483-494.

[8]Gustafson, W.A. and Pelech, I., "Effects of Curvature on Laminar Boundary Layers in Sink-Type Flow," *Transactions of the ASME, Journal of Basic Engineering*, Vol. 91, Sept. 1969, pp. 353-360.

[9]Nachtscheim, P. and Swigart, P., "Satisfaction of Asymptotic Boundary Conditions in Numerical Solution of Systems of Nonlinear Equations of Boundary-Layer Type," NASA TN D-3004, Oct. 1965.

[10]Raj. R., private communication.